Defects passivation and H-diffusion controlled by emitter region in polysilicon solar cells submitted to hydrogen plasma

S. Mahdid[a,b], D. Belfennache[c,*], D. Madi[a], M. Samah[b], R. Yekhlef[c,d], Y. Benkrima[e]

[a]*Physics of Materials and Optoelectronic Components Laboratory, Faculty of Sciences and Applied Sciences, Bouira University, P.O Box 10000 Bouira, Algeria*
[b]*A. Mira University of Bejaia, Road of Targa Ouzemour, Bejaia, 06000, Algeria*
[c]*Research Center in Industrial Technologies CRTI, P.O. Box 64, Cheraga, 16014 Algiers, Algeria*
[d]*Laboratory of Electrochemistry, Molecular Engineering and Redox Catalysis (LEIMCR) Department of Engineering Process, Faculty of Technology, Ferhat Abbas University Setif-1, Setif 19000, Algeria*
[e]*Ecole Normale Supérieure de Ouargla, 30000 Ouargla, Algeria*

A significant cost reduction in photovoltaic cells could be achieved if they could be made from thin polycrystalline silicon (poly-Si) films. Despite hydrogenation treatments of poly-Si films are necessary to obtain high energy conversion, the role of the n^+ emitter on defects passivation via hydrogen diffusion in n^+pp^+ polysilicon solar cells is not yet understood thoroughly. In this connection, influence of hydrogenation temperature and doping level of the n^+ emitter on open-circuit voltage (V_{OC}) were analyzed. It was found that V_{OC} greatly improved by a factor of 2.9 and reached up to 430 mV at a microwave plasma power and hydrogenation temperature of 650 W and 400°C, respectively for a duration of 60 min. Moreover, slow cooling is more advantageous for high V_{OC} compared to the rapid cooling. However, etching of the emitter region was observed, and this degradation is similar for both cooling methods. Furthermore, annealing of the hydrogenated cells in inert gas for 30 min revealed a slight increase in V_{OC}, which reached 40-80 mV, depending on the annealing temperature. These results were explained by hydrogen atoms diffusing into the bulk of the material from subsurface defects that are generated during plasma hydrogenation process. Also, our findings show clearly that V_{OC} values are much higher for a less doped phosphorus emitter compared to that of heavily doped. The origin of these behaviors was clarified in detail.

(Received May 20, 2023; Accepted September 14, 2023)

Keywords: Polycristalline silicon, Hydrogen diffusion, Defects passivation, Solar cells, Etching, Platelets

1. Introduction

The rapid increase in global energy demand is encouraging the development of photovoltaic energy. However, it must meet two challenges: low cost and high conversion efficiency [1-3]. These last two qualities can be achieved by referring to solar cells based on polycrystalline silicon provided that the activity of inter- and intra-grain defects is effectively passiveted by hydrogen [4,5]. To enhance the potential of thin polysilicon (poly-Si) films in photovoltaic applications, it is imperative to passivate the electrical activity of grain boundaries that results in higher energy conversion efficiency. This is commonly achieved by incorporating atomic hydrogen into the poly-Si films [6, 7]. For common solar cells, the widest hydrogenation techniques employ the immersion of n^+pp^+ cells in a dense hydrogen plasma followed by a deposition of a hydrogen-rich silicon nitride (SiN_x: H) passivation layer that serves simultaneously as an antireflection coating [8]. Despite plasma hydrogenation contributes to a large improvement in the electronic properties of thin n^+pp^+ polycrystalline silicon cells, it simultaneously induces an

* Corresponding author: belfennachedjamel@gmail.com
https://doi.org/10.15251/JOR.2023.195.535

etching of the emitter region (n^+) [9]. However, we showed in our previous works [10, 11] that microwave plasma power around 650 W involving an electron cyclotron resonance (MW-ECR) induces an efficient passivation of defects with low damage of the emitter region (n^+). But a few works reported the direct effect of the n^+ emitter region on defects passivation in hydrogenated n^+pp^+ cell structures and hydrogen diffusion in the polysilicon solar cell. However, hydrogenation conditions such as temperature, plasma power, doping level, etc., have a significant impact on the effective passivation of the defects in the poly-Si device. The understanding of kinetics behind the defect passivation by hydrogen with respect to processing conditions is very much important to form a basis for improving the efficiency of poly silicon based solar cells.

In this context, it is aimed to study the hydrogenation process of thin film polycrystalline n^+pp^+ silicon cells using MW-ECR plasma system in the present work. The influence of the substrate/hydrogenation temperature on the efficiency of defect passivation of the emitter region for its different doping level under slow and fast cooling rates as well as emitter surface etching was investigated. The passivation effectiveness was witnessed through the open-circuit voltage measured on the mesa structures of n^+pp^+ poly-Si films, while the etching process is monitored via optical interferometric microscopy and sheet resistance (R_{sq}) of the n^+ emitter region.

2. Experimental procedure

All the hydrogenation experiments were carried out using MW-ECR plasma system of the ICUBE (formerly InESS) laboratory, Strasbourg University, France. A schematic of such a system has been shown elsewhere [12]. Hydrogen gas was excited by the 2.45 GHz microwave in a resonant chamber, where a magnetic field is applied to maintain the electron cyclotron resonance (ECR) condition. The microwave plasma power was 650 W and H_2 flow was maintained at a constant rate of 30 sccm. The substrate temperature, T_H was varied from 200 to 500°C for a fixed hydrogenation time of 1 hour. The highly defective polysilicon films were produced on thermally oxidized silicon wafers by chemical vapor deposition at 1000°C using the trichlorosilane gas as a silicon precursor. The p- and p^+-silicon layers were obtained by in-situ doping with boron using hydrogen diluted diborane gas. The average thickness of the deposited p^+ and p layers is 2 µm (5×10^{19} cm^{-3}) and 5 µm (3×10^{17} cm^{-3}), respectively. A conventional diffused homojunction (HMJ) emitter was used in this work. In the HMJ process, the emitter, n^+ region is formed by thermal diffusion of phosphorus at 900°C for 30 min using doping sources such as P507, P508 and P509. This results in a distribution of P atoms according to the complementary error function (erfc) with a surface concentration ranging from 2×10^{20} to 2×10^{21} cm^{-3} and a junction depth of about 0.6 µm.

After the diffusion process, the samples were subjected to a wet chemical solution to remove the residual of dopant oxide layers. Sheet resistance of the emitter was measured using a four-point probe technique, which was in the range of 50 to 200 Ohm/sq. Side-contacted mesa structures were defined to study the performance of the solar cell device. Access to the p^+ back surface field region was made by reactive ion etching (RIE), where SF_6 gas etches the n^+p with a rate of 1.6 µm/min, thus forming a mesa cell. The samples were then loaded in the MW-ECR plasma system for hydrogenation treatments. In order to avoid the out-diffusion of hydrogen during the cooling phase, we applied two methods: the first one was a rapid cooling and the second was a slow cooling where the hydrogen plasma was maintained approximately from 10 to 20 min until the substrate temperature reaches 150°C. Finally, some hydrogenated cells were subjected to thermal annealing in the temperature range from 100 to 700°C for 30 min in a tube furnace under nitrogen (N_2) atmosphere.

3. Results and discussion

3.1. Effect of the substrate temperature

The influence of substrate temperature, hydrogenation temperature, T_H on the solar cell device parameters was studied. Fig. 1 plots the open-circuit voltage of hydrogenated n^+pp^+ mesa cells versus T_H in the range, 200 - 500 °C for a fixed microwave plasma power, hydrogen gas flux

and hydrogenation time of 650W, 30 sccm and 60 min, respectively. Thermal diffusion of phosphorus to form the emitter region n^+ was at 900°C during 60 min from doping source P507. Curve A corresponds to fast cooling after hydrogenation while curve B corresponds to slow cooling under hydrogen plasma.

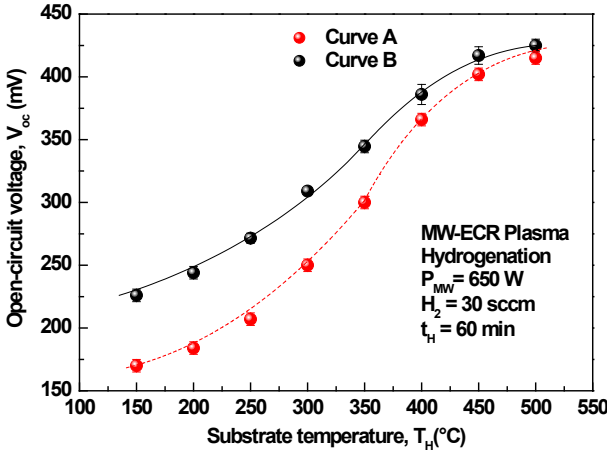

Fig. 1. Open-circuit voltage versus hydrogenation temperature measured on pc-Si n^+pp^+ mesa cells.

The curve A corresponds to rapid cooling of the samples from the plasma reactor chamber, while curve B is slow cooling, where hydrogen plasma was maintained during the cool-down phase until the T_H reached to 150°C and then removed out. The aim of such experiments (slow cooling) was to avoid the out-diffusion of hydrogen from the cells to the plasma ambiance and to trap the maximum concentration of hydrogen atoms in silicon matrix. For both operating conditions, the open circuit voltage improved drastically from 150 mV (before hydrogenation) to 430 mV after plasma hydrogenation at 450°C. This is indicative of an efficient passivation by hydrogen atoms of grain boundaries and intra-grains defects in our fine-grained poly-Si film. This could be explained by the temperature dependent diffusion constant of hydrogen atoms in silicon that led to higher diffusion lengths at higher temperatures. Above 450°C, V_{OC} began to saturate, resulting from a competition between in-diffusion and out-diffusion of hydrogen into silicon [12]. Comparison of curves A and B of figure 1 shows that fast cooling is not advantageous to achieve higher V_{OC}, especially at moderate substrate temperatures (T_H <350°C). Slow cooling could be favorable to the better incorporation of hydrogen atoms into the silicon matrix leading to slightly higher V_{OC} values compared to those obtained for rapid cooling process. According to Wilking et al. [13], higher cooling rates would reduce out-diffusion of hydrogen from silicon and result in an elevated hydrogen bulk concentration. In this case, it is important to understand why rapid cooling steps result in lower V_{OC} values compared to that obtained for slow cooling under hydrogen plasma. Assuming that improvement in open-circuit voltage is due to the passivation of defects by hydrogen diffused from the plasma but not to the defects structure change at the grain boundaries induced by temperature, the observed difference in V_{OC} values in the temperature range 200-350°C can be either due to the formation of subsurface defects as platelets [14, 15] or to the substantial etching of the n^+ emitter surface [10, 15]. As explained [14, 15], degradation of the surface and/or the generation of subsurface defects that result from the accumulation of diatomic hydrogen (H_2) located at a depth of 100 nm from the n^+ surface are harmful to the silicon based solar cells.

In order to gain a better understanding of the annealing effects on the n^+pp^+ poly-Si mesa structures, non-hydrogenated and hydrogenated at 200°C with a slow or fast cooling down were thermally annealed in the temperature range from 100 to 700°C for 30 min in a tube furnace under nitrogen (N_2) atmosphere. The measured V_{OC} with respect to cumulative annealing is plotted in Fig. 2. The hydrogenation conditions are indicated.

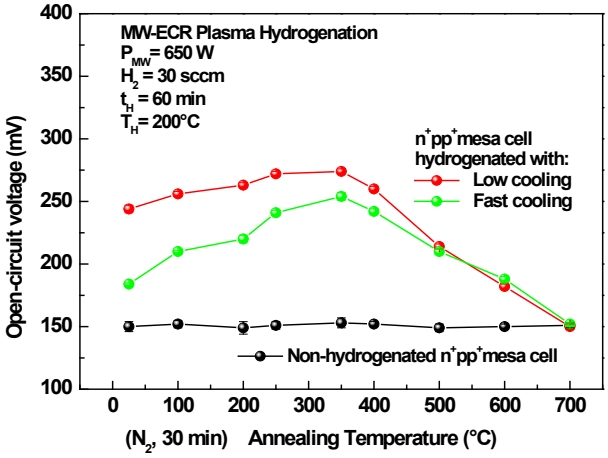

Fig. 2. Open-circuit voltage vs annealing (under nitrogen ambient) temperature of hydrogenated n^+pp^+ poly-Si mesa structures with slow and fast cooling methods.

As can be seen, for the annealing at temperatures in the range between 100 and 400°C, the hydrogenated n^+pp^+ structures with the slow cooling resulted in a little improvement in V_{OC} (ΔV_{OC} ~ 40 mV), while a significant improvement (ΔV_{OC} ~ 80 mV) is observed for rapid cooling method. However, at higher annealing temperatures, a continuous decrease in V_{OC} is observed, resulting from the out-diffusion of hydrogen from the cells. As a result, a progressive return of open-circuit voltage to its initial values could be noticed. Moreover, thermal annealing of the non-hydrogenated n^+pp^+ structures under pure nitrogen did not result in any improvement in V_{OC}. Thus, the observed increase in the open-circuit voltage is due to the passivation of defects induced by hydrogen atoms diffusing into the bulk of material from subsurface defects caused during MW-ECR plasma hydrogenation process. Measurements of the emitter sheet resistance (R_{sq}) of the n^+pp^+ structures by the four-point probe technique showed an increase by a factor of 3 to 8 after MW-ECR plasma hydrogenation for slow and rapid cooling down processes. Before hydrogenation, a sheet resistance value of 30 Ohm/sq was measured.

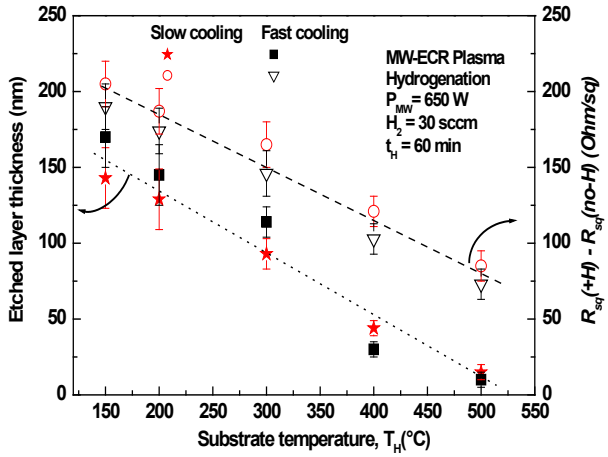

Fig. 3. Etched layer thickness and the difference in emitter sheet resistance without and with hydrogenation versus substrate temperature, T_H. The hydrogenation conditions are indicated.

In Fig.3, the etched layer thickness and the difference in emitter sheet resistance before and after hydrogenation as a function of the substrate temperature is shown. Note that a slight etching of the n^+ region was measured at higher T_H and it was accompanied with little increase in emitter sheet resistance. This result is in good agreement with the reported results [16].

These observations could be explained by referring to the literature [17, 18], where it has been confirmed that etching of the silicon surface in the presence of hydrogen plasma is a competition between electron enhanced etching of the silicon surface and redistribution of silicon from electron induced decomposition of the etch product. This usually involves the presence of hydrogen molecular H_2 on the silicon surface, via reaction between hydrogen and the silicon atoms to form an adsorbed product molecule, and finally desorption of the product molecule into the gas phase. The consequence of the above processes are largely determined by both electrons and ions energies. During hydrogenation by MW-ECR technique, the electrons in plasma act as the agents that absorb the microwave energy. The ionization of hydrogen species will occur by a collision with the energetic electrons resulting in the formation of H^+ like a dominant fraction in the plasma. Consequently, the electron and the ion H^+ energies will be low [19]. The incident ions impinging on the n^+ emitter surface in contact with plasma are usually caused by the divergent magnetic field and the sheath potential originating from the differences in ion and electron velocities. Thus, the density of the H^+ atomic hydrogen ions reaching the surface of the sample will be significant where they will be immediately converted into H^0 by reaction with electrons given by the n-type dopant in the n^+ region. At higher T_H, H^0 species have a very high diffusion coefficient with respect to the capture of an H^0 to give H_2. Therefore, it diffuses towards the p region without any Coulomb barrier to overcome. In such a case, electron induced etching via hydrogen molecules on silicon surface might be diminished. Therefore, in the present investigation, a decreasing trend of etching level with the increase of T_H was observed. However, at lower T_H , H^0 diffuses slowly and therefore the interactions with another H^0 to form H_2 on the silicon surface or in the subsurface are more important than for higher T_H , increasing each rate through a longer average time spent on the surface for the reactive species. In such a case, electron induced etching prevails, which is obvious at lower T_H in the present study as shown in Fig.3.

3.2. Effect of the doping level of the n^+ emitter region

The doping level of the emitter region also played an important role on the defects passivation in our polysilicon solar cells and the results are given in Table 1. Indeed, before hydrogenation, the results show that the open-circuit voltage (V_{OC}) of n^+p monosilicon structures (mono-Si) is not influenced by the conditions of the emitter formation in contrast to the n^+pp^+ poly-Si solar cell structures. Certainly, V_{OC} is higher for a deep emitter compared to a shallow one. This is can be explained by the fact that during emitter formation on polycrystalline films, two phenomena are responsible for improving the electrical properties of the material. One is the passivation by phosphorus of grain boundary defects and the other is removal of impurities by Getter effect from the poly-Si bulk to the inactive areas of the device [20, 21].

Table 1. Open-circuit voltage measured on monosilicon and polysilicon based solar cells for three different doping sources P507, P508 and P509. Thermal diffusion of phosphorus to form the emitter region n^+ was performed at 900°C during 60 min.

	Open-circuit voltage : V_{OC} (mV)		
Doping sources	P507	P508	P509
Mono-Si : n^+p	550 ± 10	550 ± 10	550 ± 10
Poly-Si : n^+pp^+	213 ± 5	190 ± 5	155 ± 5

After hydrogenation of the n^+pp^+ poly-Si solar cells, V_{oc} was measured as a function of substrate temperature for all the doping levels of the n^+ region. Effectively, figure 4 shows that a significant and continuous increase of V_{OC} could be observed after hydrogenation at T=450°C for 1 hour, for all the three doping sources P507, P508 and P509 used to form the n^+ emitter region. This enhancement of V_{OC} is due to hydrogen passivation of grain boundary defects and suppression of band tails that act as barriers for majority carriers and recombination sites for minority carriers. As reported in other work [22], the enhancement of the open-circuit voltage after hydrogenation is mainly due to the neutralization or passivation of the defects at the grain

boundaries and inside the grains (dislocations) of polysilicon films. This is accomplished by the fact that high doses of atomic hydrogen diffuse through the surface of the n^+ emitter into the bulk silicon from plasma environment. The latter, according to [23], is the seat of a considerable amount of H^0, H^+ and H_2

However, the measured V_{OC} values are higher for P507 than for P508 or P509. In addition, hydrogenation efficiency on the emitter doping level is more evident in terms of V_{OC} values at lower substrate temperatures (T_H <350°C), whereas at higher T_H values, the change is nominal. Indeed, at T_H = 500°C the V_{OC} is close to 440mV and for all the doping sources, while at T_H = 250 ° C, it is of the order of 339, 330 and 280 mV for doping sources of P507, P508 and P509, respectively. The results imply that the n^+ emitter region, doped with phosphorus, plays an important role in the efficiency of passivating defects in polysilicon. Also, our results are in good agreement with those reported elsewhere [24-27] wherein it was observed that hydrogen diffusion in the bulk of silicon is well prevented when the phosphorus concentration is high in the material. However, the mechanism which explains the hindrance in the diffusion of hydrogen throughout the sample is not yet properly understood. In order to accurately analyze the effect of phosphorus doping level of the n^+ emitter on the diffusion of hydrogen in the bulk of our cells, we used an approach to examine the process of phosphorus deactivation by hydrogen in monosilicon. Since monosilicon is free of defects and is easy to use as a base material for Schottky diodes, then extract the phosphorus doping profile through capacitance–voltage measurements (C-V) before and after hydrogenation of these Schottky diodes.

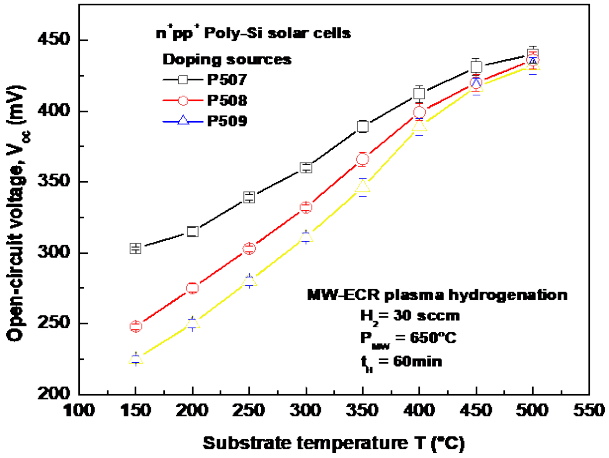

Fig. 4. Effect of the doping level of the n^+ emitter region on the open circuit voltage measured on n^+pp^+ poly-Si solar cells. The hydrogenation time is 60 min and the MW plasma power is 650 W.

The substrates used for this study are uniformly phosphorus doped [100]-oriented float zone grown monocrystalline silicon (FZ-Si) wafers with different concentrations N_p, 280µm thick and 1cm×1cm in size. Prior to hydrogenation all the silicon wafers were degreased using trichloroethylene (TCE), acetone, and methanol, treated in dilute hydrofluoric (HF) acid for removal of native oxide, then rinsed in running deionised water and finally dried into nitrogen flux. The wafers were then hydrogenated in MW-ECR plasma system. Gold contacts of 1 mm diameter were deposited using a shadow metal mask onto the hydrogenated surface, while aluminium was deposited onto the rear face to provide an ohmic contact. Then, C–V measurements were performed on the Schottky diodes at the frequency of 1 MHz and room temperature using an LCR meter (Hewlett Packard). The active donor concentration profile was extracted from these C–V measurements. The active phosphorus profiles in the Schottky diodes with starting concentrations ranging from 4×10^{14} to 4×10^{17} cm^{-3} are shown in figure 5 for the hydrogenation condition at a fixed microwave power, substrate temperature and process duration. The uniform concentrations of phosphorus in the non-hydrogenated control samples are also

shown. The data reveal that increasing the initial phosphorus concentration N_P of the samples leads to a decrease in the hydrogen phosphorus diffusion fronts Xe, representing the deep diffusion of hydrogen atoms in the bulk silicon with ($1/N_P$). We find that X_e = 0.08, 0.15, 2.75 and 11.65 µm for N_P = 4×10^{17}, 1×10^{17}, 2×10^{16} and 4×10^{14} cm^{-3}, respectively. Also, it could be observed from Figure 5 that the phosphorus deactivation rate is almost uniform over all neutralization depths. However, close to the device surface, we noticed an inclination of the doping profiles which confirms a decrease in the concentration of activate phosphorus probably due to accelerated formation of PH complexes, whereas in regions far from the surface, a slight decrease in active phosphorus concentration has been noted. It is detected that for a particular amount of hydrogen, the concentration of neutralized phosphorus in silicon is directly proportional to the concentration of phosphorus. The inactive concentration of phosphorus (N_{In}) measured at a depth of Xe in our samples as a function of initial phosphorus is shown in Fig. 6, which helps to estimate the difficulty in apparent diffusion of hydrogen. At higher concentrations of phosphorus, the N_{In} tends to saturate.

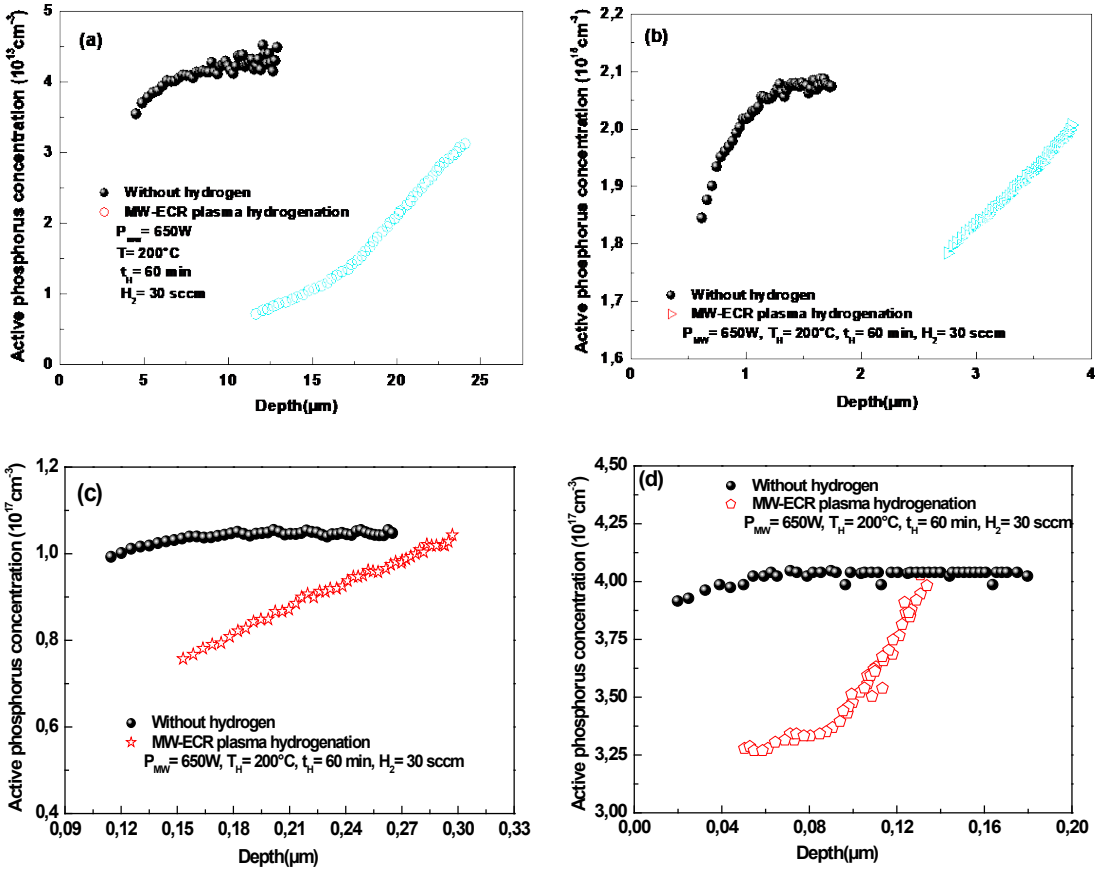

Fig. 5. Profiles of active phosphorus concentration in hydrogenated Schottky diodes on FZ-Si doped at concentrations Np: (a) $4\times10^{14}cm^{-3}$, (b) $2\times10^{16}cm^{-3}$, (c) $1\times10^{17}cm^{-3}$ and (d) $4\times10^{17}cm^{-3}$.

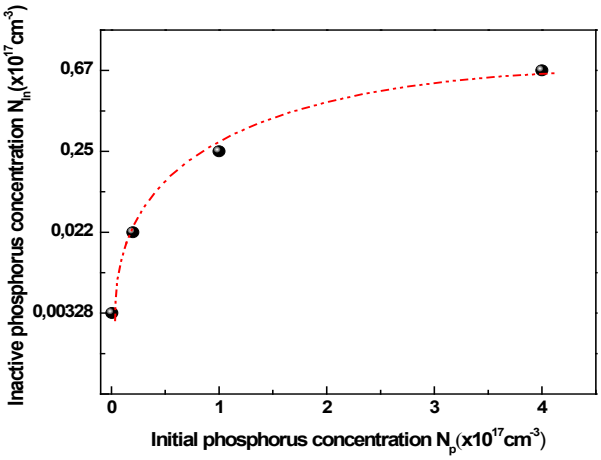

Fig.6. Inactive phosphorus concentration NIn at the depth close to Xe depending on its initial concentration Np.

The charge state of hydrogen (H^+, H^- and H^0) in silicon depends on the Fermi level position in the band gap and charge change, $H^+ \leftrightarrow H^-$, through the state configuration of H^0 as elaborated in the literature [28-30]. Furthermore, it was reported that H^0 can capture an electron or another H^0 to give respectively H^- or H_2 [28, 30]. Although, H^0 and H^- have an extremely high diffusion coefficients in n-type silicon, hydrogen could be trapped in silicon by other hydrogen atoms resulting in the formation of hydrogen molecules, H_2, located in the subsurface layer as platelets [31-33]. Because platelet nucleation occurs at phosphors sites, the increasing of phosphorus content in silicon enhances monotonically the platelet concentration [34]. Also, Huang [35] has reported the dependence of the hydrogen diffusivity upon the average size of the platelets and suggests that the in-diffusion of hydrogen is suppressed by the platelets. Consequently, H^+ absorb an electron at the sample surface to become H^0 ($H^+ + e^- \rightarrow H^0$) and the H^0 would be ionized by capturing a free electron ($H^0 + e^- \rightarrow H^-$) and then phosphorus deactivation would progress with $H^- + P^+ \rightarrow PH$. When phosphorus concentration increases, the densities of H^0 and H^- become important. This resulted in high amounts in phosphorus deactivation and larger dimension of platelets. So, the platelets impede the deep diffusion of hydrogen into the samples. However, decreasing the phosphorus concentration induces a low amount of H^- and a dispersion of H^0 on the sample surface. Therefore, the platelets amount will be little, which allows diffusion of both species H^- and H^0 as well as a deep phosphorus deactivation in silicon. To prove our arguments, we calculated the hydrogen diffusion coefficients in our samples corresponding to depth X_e through the relationship $X_e = (D_H \times t_H)^{0.5}$ where D_H and t_H are the diffusion coefficient and the hydrogenation duration, respectively. The results are listed in table 2. As already mentioned above, a high hydrogen diffusion coefficient is obtained for the samples with low phosphorus concentration, which confirms a deep penetration of hydrogen in our silicon films. These observations are in good agreement to those reported in the literature [35, 36]. Also, the values of D_H are close to those reported in the literature [36] and are consistent with their evolution.

Table 2. Calculated of hydrogen diffusion coefficients in [100]-oriented float-zone grown monocrystalline silicon wafers with different initial phosphorus concentrations

Initial phosphorus concentration N_p (atm.cm^{-3})	X_e(µm)	D_H (cm^2.s^{-1})
4×10^{14}	11.65	3.2×10^{-11}
2×10^{16}	2.75	7.6×10^{-12}
1×10^{17}	0.15	4.2×10^{-13}
4×10^{17}	0.08	2.2×10^{-13}

4. Conclusion

In this work, the effect of the n^+ emitter region on defects passivation in thin film polycristalline silicon solar cells has been studied. As a test structure, n^+pp^+ mesa solar cells were made on fine-grained polysilicon films and submitted to hydrogenation treatments. The hydrogenation is done by exposing the n^+ emitter to the hydrogen flux, which is obtained by microwave plasma discharge assisted by electron cyclotron resonance (MW-ECR). Influence of the substrate temperature under slow and rapid cooling processes on the defects passivation and emitter surface etching were thoroughly analyzed. The effectiveness of the passivation is witnessed through the changes in open-circuit voltage (V_{OC}) as measured on the n^+pp^+ mesa structures, while the surface quality is monitored via the sheet resistance (R_{sq}) and the optical morphology of the n^+ emitter region.

We found that slow cooling at the end of the hydrogenation treatments is more advantageous to achieve higher V_{OC} 's because it could be favorable for a better arrangement of hydrogen atoms into the silicon matrix, leading to a moderate higher V_{OC} value compared to rapid cooling. Also, a large improvement in the V_{OC} and a slight damage of the n^+ emitter surface has been observed at higher T_H. This is explained by considering the coexistence of both the diffusion of atomic hydrogen in the bulk of the poly-Si and the formation of platelets via molecular hydrogen, which contributes to the etching of silicon atoms once desorption molecules are produced. Indeed, as the substrate temperature decreases, hydrogen diffuses slowly and consequently, a significant increase in the density of the subsurface defects. In such a case, the defects passivation will be weak and the etching of the n^+ emitter surface will be high. At lower T_H, the hydrogen diffusion becomes even weaker and platelets density becomes, in turn, elevated. However, thermal annealing of the hydrogenated n^+pp^+ structures under nitrogen ambient provided and evidence that the subsurface defects could act as a source of hydrogen atoms for additional passivation of defects in the bulk of the cells.

As a final point, our results provide evidence that n^+ emitter region, doped with phosphorus, plays an important role in the efficiency of passivating defects in the n^+pp^+ polysilicon solar cells. In fact, we found that hydrogen diffusion in the bulk of silicon is well prevented when the phosphorus concentration is high in the material. This behavior was accurately demonstrated by phosphorus-hydrogen (PH) complexes formation in monosilicon based Schottky diodes via C-V measurements. Furthermore, our approach enabled to estimate the hydrogen diffusion coefficients in our samples, where we found that high hydrogen diffusion coefficient D_H has been obtained for samples with low phosphorus concentration.

References

[1] M. Ray, B. Chakraborty, Renew. Sustain. Energy Rev. **143**. 110884 (2021); https://doi.org/10.1016/j.rser.2021.110884
[2] Q. Cai, Q. Xu, J. Qing, G. Shi, Q-M. Liang, Energy. **261**. 125293 (2022); https://doi.org/10.1016/j.energy.2022.125293
[3] Y. Li, K. Chen, R. Ding, J. Zhang, Y. Hao, Energy Economics. **118**. 106514 (2022); https://doi.org/10.1016/j.eneco.2023.106514
[4] S. H. Lee, M. F. Bhopal, D. W. Lee, S. H. Lee, Mater. Sci. Semicond. Process. **79**. 66–73 (2018); https://doi.org/10.1016/j.mssp.2018.01.019.
[5] D. Chen, P. Hamer, M.Kim, C. Chan, A. Ciesla nee Wenham, F. Rougieux, Y. Zhang, M. Abbott, B. Hallam, Solar Energy Materials and Solar Cells. **207**. 110353 (2020); https://doi.org/10.1016/j.solmat.2019.110353.
[6] B. J Hallam, P.G. Hamer, A.M. Ciesla, C.E. Chan, B. V. Stefani, S. Wenham, Prog. Photovolt.: Res. Appl. **28 (12)**. 1217-1238 (2020); https://doi.org/10.1002/pip.3240
[7] A. El Amrani, A. Bekhtari, A. El Kechai, H. Menari, L. Mahiou, M. Maoudj, Vacuum. **120**. 95–99 (2015); https://doi.org/10.1016/j.vacuum.2015.04.041

[8] T. N. Truong, D. Yan, C. Samundsett, A. Liu, S. P. Harvey, M. Young, Z. Ding, M. Tebyetekerwa, L. Li, F. Kremer, M. Al-Jassim, A. Cuevas, D. Macdonald, H. T. Nguyen. ACS Appl Energy Mater. **2.** 8783 (2019); https://doi.org/10.1021/acsami.8b19989
[9] K. Madhavi, M. Ghosh, G. Mohan Rao, R. Padma Suvarna, J Mater Sci: Mater Electron **31**. 1904–1911 (2020); DOI: 10.1007/s10854-019-02709-8
[10] D. Madi, A. Focsa, S. Roques, S. Schmitt, A. Slaoui, B. Birouk, Energy Procedia. **2**. 151–157(2010); https://doi.org/10.1016/j.egypro.2010.07.021
[11] D. Madi, P. Prathap, A. Slaoui, Appl. Phys. A **118**. 231–237(2015); DOI: 10.1007/s00339-014-8665-z
[12] D. Belfennache, D. Madi, R. Yekhlef, L. Toukal, N. Maouche, M.S. Akhtar, S. Zahra, Semiconductor Physics Quantum Electronics & Optoelectronics **24(4)**. 378-389 (2021); https://doi.org/10.15407/spqeo24.04.378
[13] S. Wilking, S. Ebert, A. Herguth, G. Hahn, J. Appl Phys **114**. 194512 (2013); https://doi.org/10.1063/1.4833243
[14] Y. M. Pokotilo, A. M. Petuh, O. Y. Smirnova, G. F. Stelmakh, V. P. Markevich, O. V. Korolik, I. A. Svito, A. M. Saad. J. Appl. Spectrosc. **86**. 822–824 (2019); https://doi.org/10.1007/s10812-019-00900-7
[15] M. Tang, J. Ge, J. Wong, Z. Liu, T. Dippell, Z. Zhang, M. Huber, M. Doerr, O. Hohn, P. Wohlfart, A. G. Aberle, T. Mueller, IEEE J. Photovolt. **6(1)**. 10-16 (2016); DOI: 10.1109/JPHOTOV.2015.2481607
[16] D. Madi, B. Birouk, Int. J. Sci. Res. Publ. **4(4)**. 1-6(2014)
[17] H. P.Gillis, D. A. Choutov, P. A. Steiner, J. D. Piper, J. H. Crouch, P. M. Dove, K.P. Martin, Appl. Phys. Lett. **66**. 2475–2477(1995); https://doi.org/10.1063/1.114000
[18] H. F. Winters, J. Appl. Phys. **49**. 5165–5170 (1978); https://doi.org/10.1063/1.324411
[19] S.F. Yoon, K.H. Tan, Q. Zhang, M. Rusli, J. Ahn, L. Valeri, Vacuum **61**. 29–35(2000); https://doi.org/10.1016/S0042-207X(00)00429-2
[20] H. T. Nguyen, S. Mokkapati, D. Macdonald, IEEE J. Photovolt. **7**(2), 598-603 (2017); DOI: 10.1109/JPHOTOV.2017.2650561
[21] Z. Wang, Z. Liu, M. Liao, D. Huang, X. Guo, Z. Rui, Q. Yang, W. Guo, J. Sheng, C. Shou, B. Yan, Z. Yuan, Y. Zeng, J. Ye, Sol. Energy. Mater. Sol. Cells. **206**. 110256 (2020); https://doi.org/10.1016/j.solmat.2019.110256
[22] A. Slaoui, E. Pihan, I. Ka, N. A. Mbow, S. Roques, J. M. Koebel, Sol. Energy Mater. Sol. Cells **90**, 2087(2006) ; https://doi.org/10.1016/j.solmat.2006.02.004
[23] E. S. Cielaszyk, K. H. R. Kirmse, R. A. Stewart, A. E. Wendt, Appl. Phys. Lett. **67**. 3099–3101 (1995); https://doi.org/10.1063/1.114877
[24] N. H. Nickel, I. E. Beckers, Phys. Rev. B. **66(7)**. 075211 (2002); https://doi.org/10.1103/PhysRevB.66.075211
[25] D. Belfennache, N. Brihi, D. Madi, Proceeding of the IEEE xplore, 8th (ICMIC)(2016) 7804164. p. 497–502 (2017); DOI: 10.1109/ICMIC.2016.7804164
[26] D. Belfennache, D. Madi, N. Brihi, M. S. Aida, M. A. Saeed, Appl. Phys. A. **124**. 697 (2018); https://doi.org/10.1007/s00339-018-2118-z
[27] R. Ouldamer, D. Madi, D. Belfennache, Lecture Notes in Networks and Systems **591**, 700-705 (2023) Springer, Cham; https://doi.org/10.1007/978-3-031-21216-1_71
[28] C. Herring, N.M. Johnson, C.G. Van de Walle, Phys. Rev. B. 12.125209 (2001); https://doi.org/10.1103/PhysRevB.64.125209
[29] B.J. Hallam, D. Chen, M. Kim, B. Stefani, B. Hoex, M. Abbott, S. Wenham, Physica Status Solidi (a). **214 (7)**. 1700305(2017); https://doi.org/10.1002/pssa.201700305
[30] R. H. Doremus. Mat. Res. Innovat. **4(1)**. 49–59, (2000); https://doi.org/10.1007/s100190000068
[31] Y. Ma, Y. L. Huang, W. Düngen, R. Job, W. R. Fahrner, Phys. Rev. B. **72**. 085321 (2005); DOI: 10.1103/PhysRevB.72.085321
[32] C. Ghica, L.C. Nistor, B. Mironov, S. Vizireanu, Romanian Reports in Physics. **62(2)**. 329-340 (2010).
[33] E. V. Lavrov, J. Weber, Physica B, **308–310**. 151-154 (2001); https://doi.org/10.1016/S0921-4526(01)00675-5

[34] N.H. Nickel, G.B. Anderson, N.M. Johnson, G. Walker, Phys. Rev. B . **62**. 8012–8015 (2000); https://doi.org/10.1103/PhysRevB.62.8012
[35] Y.L. Huang, Y. Ma, R. Job, W.R. Fahrner, Appl. Phys. Lett. **86**. 131911–1319113 (2005); https://doi.org/10.1063/1.1896443
[36] R. Rizk, P. Mierry, D. Ballutaud, M. Aucouturier, D. Mathiot, Phys. Rev. B. **44**. 6141–6151 (1991); https://doi.org/10.1103/PhysRevB.44.6141